Linear thermal expansivity and C_p measurements for LuH_x and LuD_x ($x=0.005$ and 0.053) single crystals

C. A. Swenson
Ames Laboratory and Department of Physics and Astronomy, Iowa State University, Ames, Iowa 50011
(Received 27 March 1995)

Linear thermal expansivity (α) measurements from 1 to 300 K and heat capacity (C_p) measurements from 1 to 110 K are reported for single crystals of the α-Lu hexagonal alloys LuH_x and LuD_x ($x=0.005$ and 0.053). The C_p data confirm and extend to 110 K earlier 1 to 20 K measurements on LuH_x alloys, and, in addition, show that isotope effects, if any, are small. The small x dependences of the C_p's above 8 K can be associated with small increases in the Debye temperature Θ_0. This latter interpretation, which is consistent with ultrasonic and other results for these alloys, is valid only if C_p is expressed as mJ/g mol K (essentially, per mole of Lu ions). The present results are in agreement with the previous conclusion from more extensive polycrystalline LuH_x data that the shape of the low-temperature C_p vs T relation for $x\leqslant 0.015$ is qualitatively different from that for $x\geqslant 0.032$. The linear thermal expansivities of the c-axis alloys, even for $x=0.005$, are significantly smaller (by from 3% to 20%) than those for the pure crystals, with large isotope effects and a large, nonlinear x dependence for the low-temperature expansivity data. Other types of data have shown a feature near 170 K which is associated with the completion of pairing of the hydrogens along the c axis in next-nearest-neighbor tetrahedral sites. A distinct (approximately 15 K wide) change in α which is observed near this temperature for each alloy, except for a-axis $LuD_{0.005}$, provides the most direct evidence of such a transition. The temperature of the c-axis discontinuity is slightly isotope and x dependent, and scales approximately with x [+24% on warming for LuH(or D)$_{0.053}$]. The $LuH_{0.053}$ a-axis α's show a transition at the same temperature but of opposite sign (−15% on warming). A large relative decrease in the expansivities of each of the alloys between $T=0$ and the transition can be ascribed to a more rapid disappearance of the spin-fluctuation and electron-phonon enhancement terms for the alloys than for the pure metal. The large differences in the isotope and x dependences of the α vs T relations support the postulate that the state of these alloys is quite different for $x\leqslant 0.015$ and $x\geqslant 0.032$.

I. INTRODUCTION

The present experiments were initiated to determine the magnitude of the thermal expansivity contribution which could be associated with Thome's extensive results for the 1–20 K heat capacities (C_p) of α-phase LuH_x alloys.[1–3] In these experiments, the intrinsic C_p for high-purity lutetium was obtained using electrotransport-purified (ETP) material.[2,4] Subsequent samples (from the same starting material) were doped with H to provide alloys with from 0.57 to 15.5 at. % H ($LuH_{0.0057}$ to $LuH_{0.183}$). Previous work[5,6] had shown that H exists in single-phase solution (α- LuH_x) in Lu alloys at room temperature for concentrations of up to 20 at. % ($LuH_{0.25}$). Thome's data, which are tabulated in the original source,[1] have been published and discussed in a number of papers.[2–4,7,8] C_p data from 25 mK to 2 K which subsequently were obtained[9] for several of these samples ($x\leqslant 0.015$) show a maximum excess C_p for each sample, and also a hyperfine contribution which is important for $T<0.10$ K. Thome's results support a discussion of earlier data[10] which concludes that impurities can have a significant impact on the low-temperature C_p of Lu metal. C_p data which were taken[11] for the present Lu samples before doping with H or D agree well with those for ETP Lu, and provide assurance that the present starting material, although not of ETP quality, is of adequate purity. This preceding paper[11] gives C_p and linear expansivity results [$\alpha=(\partial \ln L/\partial T)_P$] for good-quality lutetium and scandium crystals, and an interpretation of their temperature dependences in terms of electronic effects. The Lu data published there provide $x=0$ references for the present alloy studies, and will not be repeated here.

Thome's measurements[1–3] show a low-temperature C_p anomaly which changes character and for which dC_p/dx changes sign from (+) to (−) when x increases from 0.015 to 0.032. By analogy with hydrogen and deuterium in niobium,[12,13] the suggestion was made[2,3,7–9] that the effects for $x\leqslant 0.015$ are due to tunneling of the hydrogens, presumably when bound to an interstitial such as O or N. The large tunneling contributions of H and D to C_p data for the niobium alloys, for which significant H and D differences occur,[12] are consistent with theoretical calculations.[13] Gschneidner, Gnugesser, and Neumaier[9] point out the need for LuD_x alloy data to confirm their analogy. Although low-temperature thermal expansivity results[14] do not show correspondingly large contributions due to H in niobium, tunneling often is associated with an enhanced α.[15,16] The present experiments were initiated primarily to search for such an enhanced α and its isotope dependence.

Complementary thermodynamic results for Lu have been published by Tonnies, Gschneidner, and Spedding[17] for temperature-dependent elastic constants and thermal expansions, and by Greiner, Beaudry, and Smith[18] for the effect of small amounts of H on the elastic constants. Metzger, Vajda,

and Daou[19] used energy-dispersive x-ray-diffraction measurements to determine Debye temperatures and static displacements as a function of x for LuH_x. Inelastic neutron scattering was used by Pleschiutschnig, Blaschlco, and Reichardt[20] to determine the lattice dynamics of Lu at room temperature; the dispersion relations for a $LuD_{0.19}$ alloy differ only slightly from those for pure Lu,[21] and reflect a slight hardening which is consistent with the elastic-constant results.

The state of H (D) in rare-earth (RE) solid-solution metal alloys, particularly scandium, yttrium, and lutetium, has been studied in a number of different ways, with qualitatively similar results for all three metals. The T dependences of the electrical resistivities of these alloys show a change in slope at approximately the same temperature (roughly 175 K for Lu, Ref. 22) where nuclear magnetic resonance experiments indicate a change in electronic structure.[23] The anisotropy of the transition was investigated by single-crystal $LuD_{0.183}$ resistivity measurements. These were complemented by C_p measurements from 1 to 300 K on the same material which showed a peak centered at 203 K.[24] Resistance measurements in quenching and subsequent annealing experiments show hysteresis and subsequent relaxation, from which activation energies can be determined.[22] Internal friction experiments provide complementary information.[25] Stierman and Gschneidner[8] have measured the magnetic susceptibility of Thome's samples from 1 to 300 K, and conclude that spin-fluctuation contributions are sensitive to the H content of the alloys.

Neutron scattering experiments on these alloys (see Refs. 26 and 27 for summaries) show that below 300 K the hydrogens tend to be paired along the c axis in next-nearest-neighbor tetrahedral sites which are separated by a rare-earth ion. The ''nonlabile'' or paired fraction of the hydrogens is small but significant near 300 K, increases with decreasing temperature, presumably most rapidly near the resistivity anomaly, and approaches unity near $T=0$.[27–29] The c-axis tetrahedral sites exist in close pairs between RE ions, with energy considerations not allowing adjacent tetrahedral sites to be occupied. As a consequence, these paired hydrogens exist in short chains which form an ordered pattern in the solid.[26] The potentials at these tetrahedral sites are anisotropic, with greater curvature along the c axis than along the a axis. Phonon structure which arises because of an interaction between the hydrogens in a pair has been reported for $YD_{0.17}$ (Ref. 28) and for $LuD_{0.19}$,[21] and more recently as a function of temperature for LuH_x and LuD_x, with $x\approx 0.08$ and 0.19.[30] NMR (Ref. 23) and quasielastic neutron experiments[27] (QENS) both indicate localized proton motion at low temperatures, but with different temperature dependences and a NMR time scale which is 100 times slower than that for the QENS results.[23]

Self-consistent cluster models[31,32] show that the above pairing gives the minimum energy state for H in yttrium metal, with Blaschko[33] commenting on the detailed conclusions in Ref. 31. In a plane-wave pseudopotential study of α-YH_x, Chang and Chou[34] show that the tetrahedral sites always have the lowest energy, and that pairing in these sites has the lowest energy of a number of different configurations. Min and Ho[35,36] used first-principles total-energy calculations to study $YH_{0.5}$, where one H is located at the tetrahedral site of a hexagonal unit cell. Although they do not include pairing considerations, they obtain good agreement with neutron scattering data for the magnitude and anisotropy of the H vibrational energy, and for diffusion energies. It is not clear how any of these calculations relate to the present C_p (or α) data.

II. EXPERIMENTAL DETAILS

A. Sample preparation

Gschneidner[7] has discussed in detail the preparation of high-purity RE metals. The initial Lu metal for the present samples was a 70 g polycrystalline boule, approximately 40 mm long and 15 mm in diameter. The analysis of this boule showed it to be similar in quality to Thome's starting material.[1] After this boule was heated to 1100 °C for 24 h in a vacuum of 1×10^{-8} Torr, the H concentration decreased from 0.09 at. % to less than 0.02 at. %, with no indication of the low-temperature upturn which is characteristic of H impurities. A series of C_p and inconclusive α measurements were made on this sample after successive alloying and degassing with 0.5 at. % D and 0.5 at. % H. The differences in the α data were ascribed to recrystallization in the sample upon annealing to remove the H (D) prior to preparing the next alloy. The boule then was converted to a single crystal by annealing at 1500 °C in a vacuum of 10^{-8} Torr, after which the H content was determined to be 0.010(4) at. %. Two oriented single crystals (b and c axis, each approximately 4 g with dimensions of $6\times6\times12$ mm^3) were cut from the boule and were used in subsequent experiments. (Note that, since the b- and a-axis α's are equivalent for a hexagonal crystal, this crystal, for convenience, will be designated an a-axis crystal in the following.) The good agreement at all stages[11] between C_p's for the present (degassed) starting material and Thome's results[1] suggests that, for practical purposes, this material was equivalent to his ETP samples.

The polycrystal and single-crystal H (D) alloys were prepared by heating the electropolished sample to 700+ °C in a glass high-vacuum system to break down the oxide layer before a titrated amount of H or D was added to the vacuum system. The pressure in the system dropped quickly as the gas was taken up by the 700 °C sample. The sample then was kept at 650–700 °C in high vacuum for a week to homogenize the H (D). Vacuum fusion analysis samples were taken from the polycrystal after each procedure (alloying and subsequent degassing), as was done by Thome,[1] with the boule's final mass decreased from 70 to 50 g. This sampling procedure was not practical for the single crystals, since each of the small samples was used for a number of different H (D) alloys. Instead, the H (D) content of a sample was assumed to be given by the mass of the gas absorbed by the sample. This was verified by comparing the initial and final masses of the crystal.

A puzzling aspect of the present experiments is that the degassing of a $LuH(D)_x$ alloy at 1050–1100 °C and 10^{-8} Torr usually did not decrease the H (D) content below approximately 0.1 at. % ($x\approx0.001$); the initial degassing of the bulk crystal was an exception. A H content of this magnitude can seriously affect low-temperature C_p data, since Thome's data[1] for $LuH_{0.000\,35}$ (0.035 at. %) show an excess C_p of approximately 5% near 1 K. As a test, just prior to carrying out

the single-crystal growth procedure, the large polycrystal was held at 1070 °C for 33 days in a vacuum which ultimately reached 3×10^{-9} Torr. The levels of the gaseous impurities, including H (final concentration 0.08 at. %), essentially were unchanged by this procedure. The temperature of Lu metal apparently must be (significantly?) greater than 1100 °C to remove H (D) quantitatively. Whether these observations apply to H (D) alloys of yttrium, scandium, and other RE metals is not known.

The order in which data were obtained for the various alloys was as follows. The pure *a*- and *c*-axis samples were combined for a C_p measurement before determining the individual α's. C_p and α data then were taken for the same crystals after successive alloying and degassing. The sequence for the *c*-axis crystal was as follows: $LuH_{0.005}$, $LuD_{0.005}$, $LuD_{0.0002}$ (the degassed previous sample), $LuD_{0.053}$ (5 at. % D), and $LuH_{0.053}$. The initial *a*-axis alloy, $LuD_{0.005}$, showed very small changes in α, so no *a*-axis $LuH_{0.005}$ alloy was prepared (the *c*-axis $LuD_{0.005}$ alloy had shown much greater effects than $LuH_{0.005}$). This processing was carried out over a period of years using the same apparatus and techniques, so the samples are believed to be as equivalent as possible. Unfortunately, the *a*-axis sample was destroyed in attempting to form a $LuH_{0.053}$ alloy. Since the original crystal material no longer was available, a second, larger, *a*-axis sample (0.04 vs 0.02 mol) was cut from a different Lu single crystal which was of comparable purity (analysis showed 0.02 at. % H, near the limit of detection). Rather extensive C_p data (but no α's) taken for this starting material agreed well (better than $\pm0.5\%$ at all T's) with the more limited original combined-crystals data, and also with the degassed *c*-axis sample data above 3 K, with no indication of a low-temperature H-related upturn.[11] This sample then was alloyed to form $LuH_{0.053}$, and both C_p and α data were taken.

After the rather spectacular expansivity data for $LuD_{0.005}$ (see below) were obtained, a possible interpretation was that the sample had become polycrystalline when it was degassed and then alloyed with D. A neutron-diffraction characterization of the sample[37] confirmed, however, that it was a single crystal, with its longest dimension corresponding to the *c* axis.

B. Calorimetry and dilatometry

Heat capacities were measured from 1 to 110 K using a conventional heat-pulse tray calorimeter, with Apiezon-N grease providing contact between the sample and the copper tray. A single calibrated[38] germanium resistance thermometer was used for temperature measurements. A mechanical heat switch provided thermal contact between the tray and an isothermal shield; no exchange gas came into contact with the sample at any time. The ratio of the sample heat capacity to the addenda heat capacity was greater than 3 at 1.3 K, 1.5 at 4 K, and 0.5 at 80 K. The precision of the C_p data (related to the scatter of the data) was roughly $\pm0.3\%$ above 4 K; comparisons with other data[11] suggest an absolute accuracy of roughly $\pm0.5\%$ up to 40 K, rising to $+1.5(5)\%$ above 80 K where the temperature scale is not well documented. A comparison of the initial single-crystal data with those for the *c*-axis sample after degassing following the $LuH(D)_{0.005}$ runs shows $\pm0.4\%$ agreement from 2.5 to 80 K; Thome's data[1] were used to estimate the D concentration for this sample ($x=0.0002$, or 0.02 at. % D) using the slight (1.3%) C_p excess which appears below 2 K. These data also were in similar agreement with those for the new *a*-axis crystal.

The above estimates of reproducibility probably are too optimistic for the alloy samples. The C_p data for the *a*- and *c*-axis $LuD_{0.005}$ alloys agree to better than 1% above 5 K, but differ by 2(1)% below 4 K; the *c*-axis $LuH_{0.005}$ data lie between these. The C_p data for the *a*-axis $LuH_{0.053}$ sample differ systematically from those for *c*-axis $LuH_{0.053}$ (see below); the data for this ''new'' sample are 3(1)% smaller below 4 K; and $+1.5(5)\%$ larger from 10 to 80 K. The *c*-axis $LuD_{0.053}$ data are intermediate between these. The agreement between C_p's for the new *a*-axis crystal (prealloying) and other pure data shows that sample size is not a factor. The new alloy was prepared in a different facility, using different procedures, which possibly could have affected the state of the alloy. In particular, this sample initially was annealed for only 24 h before C_p data were taken. When the differences with the corresponding *c*-axis sample were noted, the sample was removed from the calorimeter, sealed in quartz, and reannealed at 700 °C for 8 days. The resulting C_p data were indistinguishable from those first taken ($\pm0.2\%$), which indicates that alloy inhomogeneities should not be a problem in either this or previous work. These relatively small discrepancies, which could be associated with the earlier data, suggest caution in comparing results for different samples which, presumably, are, or should be, identical.

The linear thermal expansivities $[\alpha=(1/L)(\Delta L/\Delta T)=(\partial \ln L/\partial T)_P$ for small $\Delta L]$ of these 12-mm-long single crystals were determined from 1 to 300 K using a variable-sample-length differential capacitance dilatometer.[39] All data were taken isothermally (T constant to 1 mK); capacitance readings subsequent to a change in T (which could be as small as ±0.5 K or as large as ±20 K) were taken only after capacitance drift (presumably due to T differences between the sample and the dilatometer) was negligible. Equilibrium times (in the absence of sample effects) varied from one hour near room temperature to a few minutes below 10 K. The absolute accuracy of these measurements is approximately $\pm1.5\times10^{-9}$/K at low temperatures ($T<20$ K for the *a*-axis and $T<7$ K for the *c*-axis crystals) and $\pm0.5\%$ at higher temperatures. The internal consistency of the data (the larger of $\pm5\times10^{-10}$/K or $\pm0.2\%$) is much better than this for a given run, with uncertainty in the magnitude of the correction for the cell ''expansion'' (determined with respect to a pure copper sample) a major source of systematic error.

C. Data analysis and presentation

The methods which were used to analyze and present these data are described in detail in the paper describing the pure-crystal results,[11] and will not be repeated here. At low temperatures, C_p and α for a pure metal are expected to follow the same temperature dependence, with,

$$C_p/T=\sum_{n=0}^{N} C_n T^{2n} \tag{1a}$$

and

$$\alpha/T=\sum_{n=0}^{N} A_n T^{2n}. \tag{1b}$$

In the limit as $T\rightarrow 0$, these suggest the conventional C_p/T (or α/T) vs T^2 plot of the data. The C_0 and A_0 parameters are associated with electronic contributions, while the C_1, A_1, and higher-order parameters are associated with the lattice. In particular, $C_0=\gamma$, the electronic C_p coefficient, while C_1 is related to the limiting lattice Debye temperature Θ_0 by

$$\Theta_0=\{[1.944\times 10^6 \ \ (\text{mJ/g mol K})]/C_1\}^{1/3} \ \ \text{K}. \tag{2}$$

Low-temperature deviations from linearity in these plots imply an anomalous contribution to C_p (α). At higher temperatures, power series including all powers of T can be used more effectively to represent both C_p and α, with the coefficients having no physical significance.[11]

Experimental data $C_p(T_i)$ (where T_i represents an individual data point) can be presented quite sensitively for a wide range of temperatures using temperature-dependent equivalent Debye Θ's to represent parametrically the lattice contribution $C_p^{\text{lat}}(T_i)$. $\Theta(T_i)$ is defined by the relation

$$C_p^{\text{lat}}(T_i)=C_p(T_i)-C_p^{\text{elect}}=C_p-\gamma T_i=C_D[T_i/\Theta(T_i)], \tag{3}$$

where $C_D(T/\Theta)$ is the Debye function.[40] $\gamma(C_0)$ is obtained from a fit of Eq. (1a) to the low-temperature data, which also gives C_1 and, hence, Θ_0 [Eq. (2)]. For a Debye solid, $\Theta(T_i)=\Theta_0$, while for a real solid Θ typically decreases to a minimum with increasing T, and then varies only slowly with temperature. If the volume (or, for the present data, concentration) dependence of the lattice entropy or C_p can be described in terms of a characteristic temperature Θ_0, the data for alloys with different x should coincide in a reduced plot of the data, $\Theta(T_i)/\Theta_0$ vs T_i/Θ_0, where $\Theta_0(x)$ [or $\Theta_0(V)$] is an adjustable parameter. For sufficiently ''high'' temperatures ($T/\Theta_0>0.05$, or 10 K, for Lu), this type of plot is relatively insensitive to small ($\pm 10\%$) variations in γ.

The C_p's and single-crystal α's are related through the Grüneisen relations, which involve the elastic constants and molar volumes.[11] The resulting Grüneisen parameters have significance only if the various contributions to the thermodynamic properties (electronic, lattice, etc.) can be unambiguously separated. While this can be accomplished reasonably well for the pure-crystal data, the large impurity effects for the α's of the present alloys make such an analysis impractical.

III. RESULTS AND DISCUSSION

Since, contrary to expectation, no definitive relationship exists between the experimental C_p and α results for the present six alloy samples, the C_p and α data will be discussed separately. This lack of a relationship perhaps is related to the results for the pure crystals[11] which show that electronic effects are much more significant for the principal-axis α's than for the C_p's. The pure Lu reference functions used in the present paper are those which are described in the pure-crystal paper.[11]

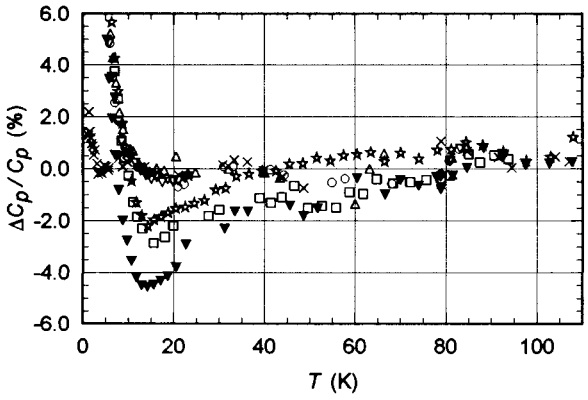

FIG. 1. Relative differences between the various alloy C_p data and those for pure Lu; c-axis degassed $LuD_{0.0002}$ ($\times$), c-axis $LuH_{0.005}$ ($\triangledown$), c-axis $LuD_{0.005}$ ($\bigcirc$), a-axis $LuD_{0.005}$ ($\triangle$), c-axis $LuH_{0.053}$ ($\blacktriangledown$), c-axis $LuD_{0.053}$ ($\square$), and a-axis $LuH_{0.053}$ ($\star$).

A. C_p results

The C_p data for both alloy concentrations initially were analyzed in terms of the gram atomic weights [mJ/(g at.) K] of the samples, following Thome.[1] For the alloys with $x=0.053$ (5 at. %), this definition results in C_p's above 60 K which are approximately 5% smaller than those for the pure material. At these temperatures, the total electronic contribution to C_p is less than 3% (it is most important below 10 K), so this difference cannot be related to electronic effects, but must be associated with the lattice, and an increase in Θ [Eq. (3)] of from 10 to 15%.[11] This conclusion can be compared with direct determinations of the change in Θ with x for Lu alloys. The ultrasonic results of Greiner, Beaudry, and Smith[18] show $d\ln\Theta_0/dx=0.3(1)$ for $0.005\leqslant x\leqslant 0.0069$, while Metzger, Vajda and Daou[19] used dispersive x-ray diffraction to obtain $d\text{Ln}\Theta_\infty/dx=0.46(8)$ for $0.014\leqslant x\leqslant 0.133$ (Θ_∞ is the limiting, high-T value of Θ; see Ref. 11). These results would predict a much smaller (2%) increase in Θ, or a decrease in C_p of less than 1%. When the assumption is made that the H (D) is firmly bonded to a Lu ion (as the pairing model suggests) and C_p is calculated for one gram molecular wt (essentially, for one mole of Lu ions), the C_p results above 60 K are identical to better than $\pm 1\%$ (see below) for all alloys. For consistency, Thome's original data,[1] where they have been used in the following, have been recalculated to reflect this definition.

With this definition, the present results for $T>10$ K (Fig. 1) differ only slightly from those for pure Lu metal.[11] The data for the three samples with $x=0.005$, and for the degassed sample, agree among themselves and with the pure-metal relation to $\pm 0.5\%$ above 10 K. The systematic differences from the pure metal C_p's which occur between 10 and 30 K for the three samples with $x=0.053$ [$-3.2(10)\%$ near 15 K] can be described by a slight [1.3(5%)] increase in Θ_0; the temperature dependence of these differences is consistent with that which would be expected for this change in Θ_0 and is not consistent with a decreased γ for these alloys. The slight low-temperature upturn of the data for the degassed sample in Fig. 1 ($\times$) reflects an estimated 0.02% D content.

The low-temperature region ($T<20$ K) is shown in greater detail in Fig. 2; the y-axis scale for the lower part is

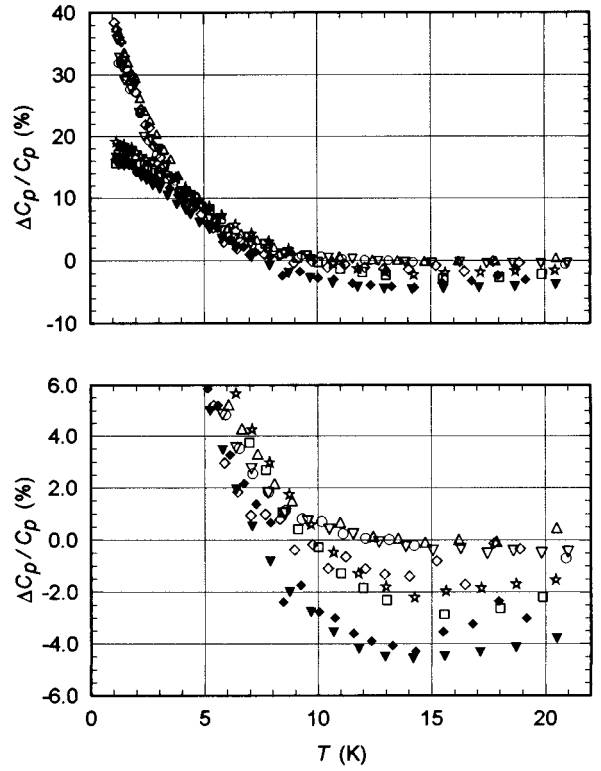

FIG. 2. Relative differences between the various 1–22 K alloy C_p data and those for pure Lu. The symbols for the crystal data are as in Fig. 1. The differences from the smooth ETP relation also are shown for Thome's (Ref. 1) polycrystalline $LuH_{0.0057}$ (◇) and $LuH_{0.065}$ (◆) data.

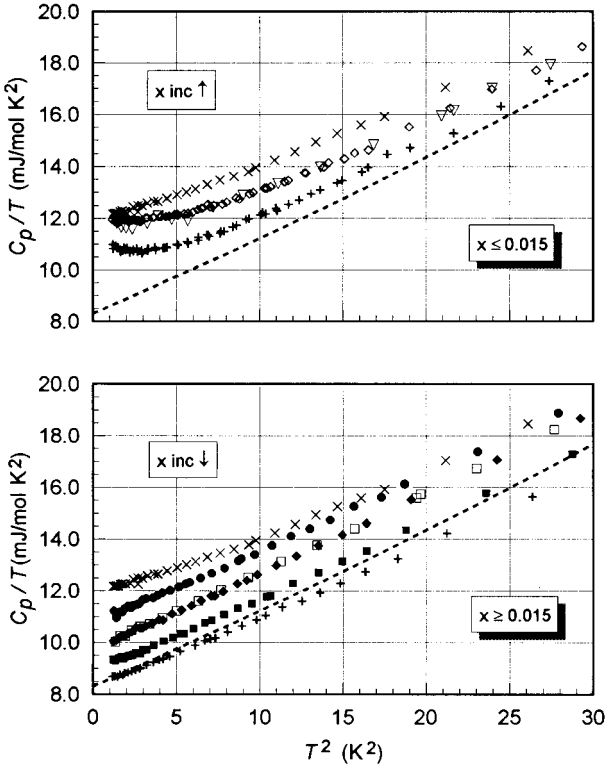

FIG. 3. C_p/T vs T^2 plots for selected data. Unless otherwise noted, the symbols refer to the polycrystalline alloy data (Ref. 1). Both parts: pure Lu (----), $LuH_{0.015}$ (×). "$x \leqslant 0.015$:" c-axis $LuH_{0.005}$ (▽), $LuH_{0.0022}$ (+), and $LuH_{0.0057}$ (◇). "$x \geqslant 0.015$:" $LuH_{0.032}$ (●), c-axis $LuD_{0.053}$ (□), $LuH_{0.065}$ (◆), $LuH_{0.124}$ (■), and $LuH_{0.183}$ (+). The c-axis $LuD_{0.005}$ and a-axis $LuD_{0.005}$ data bracket the c-axis $LuH_{0.005}$ data shown; similarly, the c-axis $LuH_{0.053}$ and a-axis $LuH_{0.053}$ data bracket the c-axis $LuD_{0.053}$ data.

the same as for Fig. 1, while the upper part has an extended scale to include the lowest-temperature data. Thome's results[1] (as differences from a fit to his ETP data) are given in Fig. 2 for the two values of x (0.0057 and 0.065) which are closest to those for the present samples. For temperatures above 5 K, the lower part of Fig. 1 shows better than ±0.5% agreement between the various lower-x crystal data, with poorer consistency (slightly more than ±1%) between the higher-x data. The differences between the a-axis and c-axis $LuH_{0.053}$ C_p's are unexpectedly large and extend almost to 80 K (Fig. 1); they possibly reflect differences in the preparation of the two samples.

The upper part of Fig. 2 shows two distinct features of the low-temperature (below 3 K) C_p results for these alloys; in agreement with Thome's results,[1–3] the C_p's are systematically greater for $x=0.005$ than for $x=0.053$, and, in addition, do not show a distinguishable isotope effect. At 2 K, the differences from the pure metal C_p [$\Delta C_p/C_p = 28.5(1.5)\%$ for $x=0.005$ and 17(1.5)% for $x=0.053$] show a scatter which is not systematic with H or D, and which is approximately the same for the two values of x. Within these limits, Thome's polycrystal results for $LuH_{0.0057}$ and $LuH_{0.065}$ are indistinguishable from the present $x=0.005$ and 0.053 data, respectively. Our early data for alloys of the large (>50 g) polycrystalline sample ($LuH_{0.0049}$ and $LuD_{0.0054}$, not shown) gave consistent but smaller C_p's, with $\Delta C_p/C_p = 20.5(1.5)\%$ at 2 K. The implication is that for $x=0.005$ the C_p's are a maximum for small single crystals, possibly are smaller for similarly sized polycrystals, and are appreciably smaller for the large polycrystal. The significance of this observation, which may be fortuitous, is not obvious, however, H possibly is trapped in the grain boundaries of the polycrystals.

The two parts of Fig. 3 present the C_p results for $LuH(D)_x$ alloys using the conventional C_p/T vs T^2 representation [Eq. (1a)]. A number of Thome's LuH_x results[1] are included also to emphasize the contrasting x dependences for $x \leqslant 0.015$ ($dC_p/dx > 0$) and $x \geqslant 0.015$ ($dC_p/dx < 0$). The agreement between the present (isotope-independent, not shown) results and those of Thome for $x=0.0057$ and 0.065 is evident in these figures; the "pure" relationship (the dotted curve) represents equally well the pure crystal and the ETP data. The $LuH_{0.015}$ results are given in both parts to emphasize that a maximum in the anomaly presumably occurs for $0.015 \leqslant x < 0.032$. As in Fig. 2, the shapes of the curves in Fig. 3 are qualitatively different for $x \leqslant 0.015$, where each shows an upturn at low T, and for $x \geqslant 0.032$, where each can be represented by a linear relation. The coefficients for this linear relation [Eqs. (1a) and (2)] are given in columns 3 and 4 of Table I for the pure samples,[11] and for the $x \geqslant 0.032$ alloy data. While the γ's for the $x \geqslant 0.032$ alloy data show a consistent decrease with increasing x, the x dependence of the Θ_0's is somewhat erratic.

TABLE I. Parameters for fits of Eq. (1a) to the data in the lower part of Fig. 3, and for the normalizations of the reduced Θ/Θ_0 vs T/Θ_0 relation (Fig. 4). γ is given in units of mJ/mol K^2, Θ_0 in K.

Sample		Low-T fit		Normalized Θ_0[a] Fit γ	Pure γ
Alloy	x	γ	Θ_0	Θ_0	Θ_0
Pure crystal	0.000	8.299	189.91	189.91	189.91
Lu c + D	0.053	9.770	189.1	192.5	191.9
Lu c + H	0.053	9.715	193.8	193.3	192.8
Lu a + H	0.053	9.939	189.0	191.5	191.0
ETP	0.000	8.303	190.03	190.03	190.03
Thome, LuH_x	0.032	10.776	194.9	193.1	191.3
Thome, LuH_x	0.065	9.734	189.8	193.5	192.5
Thome, LuH_x	0.124	8.886	192.9	196.2	195.5
Thome, LuH_x	0.183	8.280	196.5	198.2	198.0

[a]See Fig. 4.

Figure 4 contains reduced plots of the lattice C_p relation [$\Theta(T_i)/\Theta_0$ vs T_i/Θ_0, see Eq. (3)] for $x \geq 0.032$ for the present data (upper) and for Thome's data (lower). The dashed-line reference relations in Fig. 4 represent the smooth fits to either the pure-crystal results[11] (upper) or to the ETP data[1] (lower). For the alloys, the "fit" value of γ (col. 3, Table I) was used to calculate the lattice C_p's and corresponding equivalent Θ's [Eq. (3)] from the data for each of the alloys. The value of $\Theta_0(x)$ was adjusted manually until the reduced Θ's coincided with the pure metal relations, as is shown in Fig. 4. The lower-temperature limit for this procedure was chosen to be 0.04 (approximately 7.6 K), since uncertainties in γ could have a significant effect at lower temperatures; the upper limit was determined arbitrarily by the onset of scatter in the crystal data above 45 K, and by the upper limit of Thome's data (20 K). The excellent agreement between the data and the $x=0$ relations for these temperatures [± 0.003 in $\Theta(T_i)/\Theta_0$] reflects directly the x-independent shape of the alloy lattice C_p relations. The resulting Θ_0's, which are given in col. 5 of Table I, show more consistency than those obtained from the low temperature fits to the data.

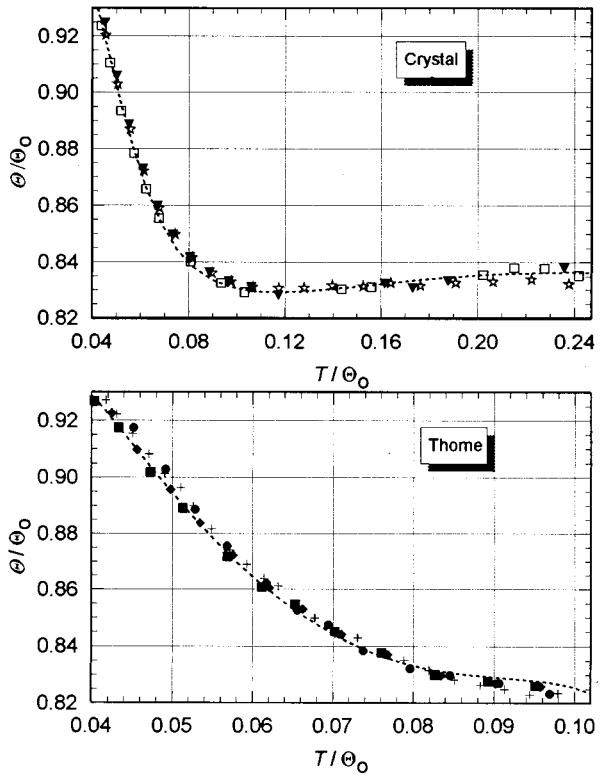

FIG. 4. Normalized, Θ/Θ_0 vs T/Θ_0, plot of the lattice C_p's for alloys with $x \geq 0.032$. See the text for details. The crystal alloys are as in Fig. 1, while Thome's alloys are as in Fig. 3. Lattice C_p's were calculated using the "low-T fit" γ's in column 3 of Table I; the Θ_0's used for the normalization are in column 5 of Table I.

This procedure was repeated for each alloy using the (usually) smaller pure value of γ in column 3 to investigate the effects of variations in γ. The representations (not shown) were equally satisfactory, and correspond to the Θ_0's which are given in column 6 of Table I. The smaller magnitudes of these Θ_0's correspond to the slightly larger lattice C_p's associated with the use of $x=0$ γ's. The relative change in Θ_0 with x which follows from both of these procedures, $dLn\Theta_0/dx = 0.23(4)$, is in reasonable agreement with the ultrasonic [0.3(1)][18] and x-ray [0.46(8)][19] results. The good agreement from 10 to 100 K between the pure metal and various $x=0.005$ crystal data (Figs. 1 and 2) is consistent with a negligible x dependence in Θ_0 for these dilute alloys.

B. Expansivities

Figure 5 shows the temperature dependences of the α's for pure single-crystal Lu metal (the dotted and dashed lines), and for the six alloys (the symbols). The data for both the c- and the a-axis crystals are given in the upper part of Fig. 5 to show the magnitude of the anisotropy in the α's, while the lower part presents on an expanded scale only the a-axis data. A striking feature in these (and the following) plots is their distinct contrast to the C_p results; the c-axis α is very sensitive to small amounts of D [it is decreased by from 10% to 20% upon alloying with 0.5% D (or 5.0% H or D)], with a very significant isotope effect for $x=0.005$. The rapid change in α near 170 K for each of the alloys suggests

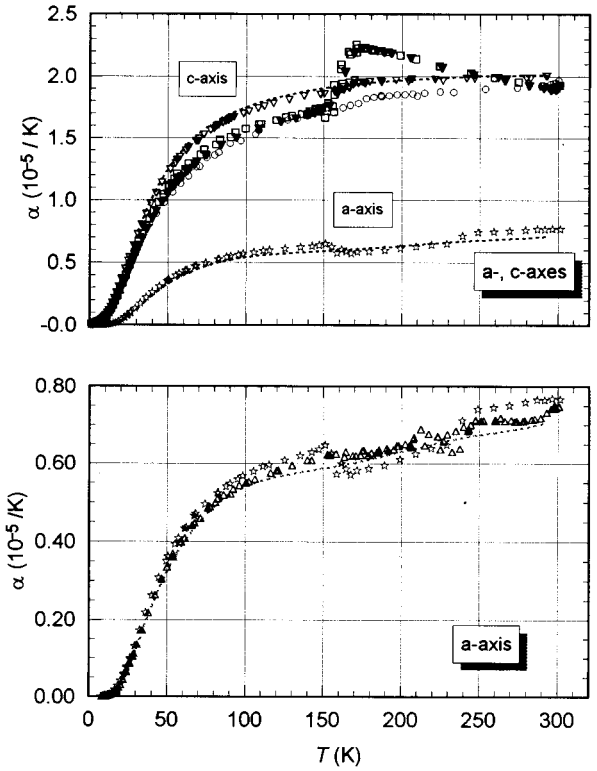

FIG. 5. α vs T relations for pure Lu (----) and Lu alloys. c axis: $LuH_{0.005}$ (▽), $LuD_{0.005}$ (○), $LuH_{0.053}$ (▼), and $LuD_{0.053}$ (□). a axis: $LuD_{0.005}$ (△) and $LuH_{0.053}$ (☆). Note the vertical scale differences.

a transition which undoubtedly is associated with the completion of the pairing of H or D in next-nearest-neighbor sites along the c axis. The change in the a-axis $LuH_{0.053}$ α's near 230 K is a real effect which does not appear in the corresponding c-axis data; its origin is not understood. The data for both this alloy and for the a-axis $LuD_{0.005}$ alloy show appreciably more hysteresis and scatter above 150 K than the c-axis alloys.

The transition temperatures T_{tr} are defined as the midpoints of these relatively broad transitions. The transition temperatures, their widths, and the fractional changes in α at the transition are summarized in Table II for each alloy, together with other published data for T_{tr}. Since the a-axis and c-axis alloys show differences from the pure metal of opposite sign, the relative effects on the volume expansivities (not shown)

$$\beta=(\partial \ln V/\partial T)_P=\alpha_c+2\alpha_a \tag{4}$$

are significantly smaller (by a factor of approximately 2) than those for the linear expansivities.

In Fig. 6, the α/T vs T^2 plot of the low-temperature portion of these data (compare with Fig. 3) shows that the differences in Fig. 5 persist to the lowest temperatures, Here, the solid line in each figure represents the smooth pure-crystal expansivities, while the various dashed and dotted lines represent fits of Eq. (1b) to the corresponding data; the low-temperature intercept for each of these fits (A_0) is given in the first line of Table III. The behavior of the c-axis data in Fig. 6 resembles qualitatively that of the corresponding data in Fig. 5, with $LuH_{0.005}$ differing only slightly from the pure metal, in contrast with the relatively common behavior (and decreased magnitudes) for the other three crystals. The data which are shown for the degassed c-axis crystal agree well with the initial pure-crystal relation. The a-axis α's are an order of magnitude smaller than those for the c axis (note the vertical scale difference), with quite different behavior for each of the two samples. An important difference between Fig. 3 and Fig. 6 is that the α plots for $x=0.005$ do not show the same upturn at low temperature as those for C_p. This most likely reflects a lack of sensitivity in the α determinations.

Figure 7 presents the c-axis data of Fig. 5 more sensitively as the ratio of the alloy α's to those for the pure metal at the same temperature; a similar plot for the a-axis α's is not useful since $\alpha_{pure}=0$ near 10 K. The low-temperature knee in these plots (especially for $x=0.005$) occurs near temperatures where electronic contributions (proportional to T) become significant. Changes in electronic properties are emphasized by the difference $(\alpha-\alpha_{pure})/T=\Delta\alpha/T$ which is plotted vs T in Figs. 8 (c axis) and 9 (a axis) for the various

TABLE II. Transition parameters. T_{tr} is defined as the midpoint of the transitions in Figs. 5 and 7–9; the uncertainties reflect transition widths. The resistivity transitions appear to have similar widths.

	T_{tr} (K)		$\Delta\alpha/\alpha$ (%)		
Sample	H	D	H	D	Comments
c axis					
$x=0.005$	167(5)	178(6)	2.5(5)	2.1(3)	
$x=0.053$	163(7)	159(7)	24(1)	24(1)	
a axis					
$x=0.005$		170(10)		−1.4(10)	poorly defined
$x=0.053$	160(8)		−15(1)		
Resistivity					
$0.04\leqslant x\leqslant 0.235$	172				Ref. 41
$0.05\leqslant x\leqslant 0.19$	166	172			Ref. 22
$x=0.183$		174.(5)			Single crystal, Ref. 24
C_p					
$x=0.183$		203(20)	$\Delta C_p/C_p=0.03$		Single crystal, Ref. 24

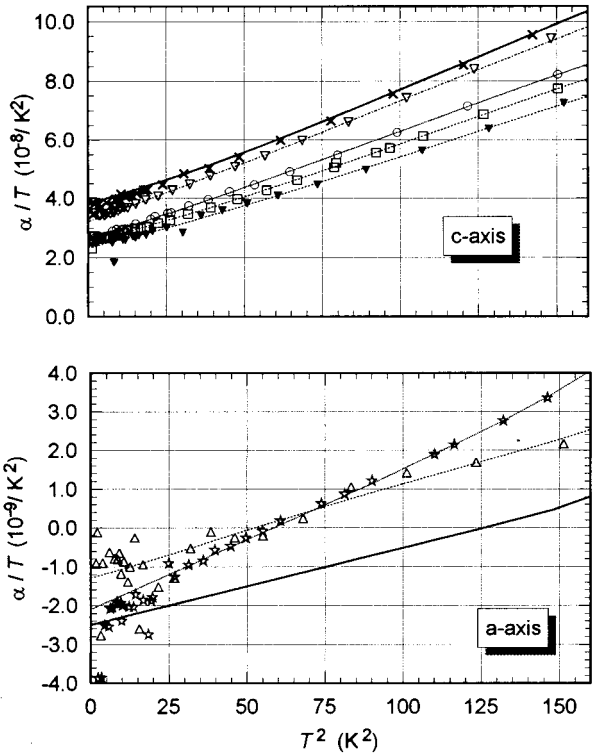

FIG. 6. α/T vs T^2 plot for pure Lu (—) and Lu alloys; the alloys are as in Fig. 5, with the addition of the degassed *c*-axis sample $LuD_{0.00021}$ (×) (see Figs. 1 and 2). The various dashed and dotted lines represent smooth fits to the data through which they pass. Note the vertical scale differences.

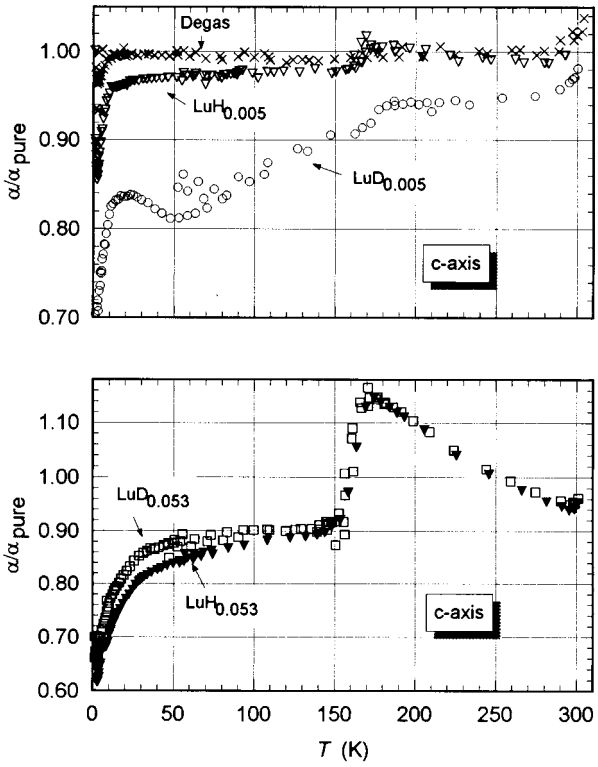

FIG. 7. The ratio of *c*-axis alloy expansivities to those for the pure metal, $\alpha/\alpha_{\text{pure}}$. The alloys are as in Fig. 6. Note the vertical scale differences.

alloy data. The dotted curves in each of these figures relate $\Delta\alpha$ to α_{pure}, with magnitudes which correspond to $\alpha_{\text{pure}}/10T$.

A common feature of the four *c*-axis relations in Fig. 8 is the approximate correspondence between $\Delta\alpha/T$ at $T=0$ and at the low-temperature end of the transition, with a significant intermediate minimum. The temperature of this minimum varies from 30 K for $x=0.053$ (no isotope nor orientation effect) to 35 K for *c*-axis $LuH_{0.005}$ and 50 K for *c*-axis $LuD_{0.005}$. The shapes of these curves qualitatively mirror the shape of the lattice thermal expansivity, when the assumption is made that α/T is constant for the electronic contribution. For temperatures greater than T_{tr}, α is unchanged for *c*-axis $LuH_{0.005}$, but is decreased by approximately 6% for *c*-axis $LuD_{0.005}$. The α's for the *c*-axis $x=0.053$ alloys are smaller than those for the pure metal near 290 K (comparable with those for $LuD_{0.005}$) but increase rapidly with decreasing T and do not show a significant isotope effect.

The *a*-axis alloy plots in Fig. 9, when compared with the more extensive *c*-axis data in Fig. 8, show comparable general features, but a larger scatter of the data (note the order-of-magnitude more sensitive scale) and, for $LuH_{0.053}$, greater structure. T_{tr} is poorly defined for $LuD_{0.005}$, although $\Delta\alpha/T=0.10(5)\times10^{-8}/\text{K}^2$ above approximately 170 K, and $0.15(5)\times10^{-8}/\text{K}^2$ for lower temperatures. The large scatter in these $LuD_{0.005}$ data appears because all of the data for this sample are plotted, with no distinction between the several different warming and cooling runs which were internally consistent (to better than ±0.5%), but which showed considerable hysteresis; the negative spike at 230 K (−5%) occurred on a final warming run, while the subsequent cooling run gave the positive spike at 210 K (+6%). The $LuH_{0.053}$ data in this figure are those for the final warming run after the sample had been cooled to 1 K. The original cooling run is similar in shape, but somewhat different in magnitude. While the 15% decrease in α at 160 K can be associated with the 24% increase at 163 K for the *c*-axis crystal, there is no comparable feature in the *c*-axis data which can be related to the 10% increase in the *a*-axis α near 240 K. The negative spike on warming for the $x=0.005$ crystal and this feature occur at the same temperature, and reflect effects which ap-

TABLE III. The leading parameter for Eq. (1b) for fits to the data of Fig. 6. A_{0b} is the "high-temperature" (bare density of states) value for pure Lu (Ref. 11).

	a axis			*c* axis				
Sample	Pure	0.005D	0.053H	Pure	0.005H	0.005D	0.053H	0.053D
A_0 (10^{-08}/K)	−0.25	−0.13	−0.21	3.82	3.2	2.6	2.3	2.5
A_{0b} (10^{-08}/K)	0.50(5)			−0.3(2)				

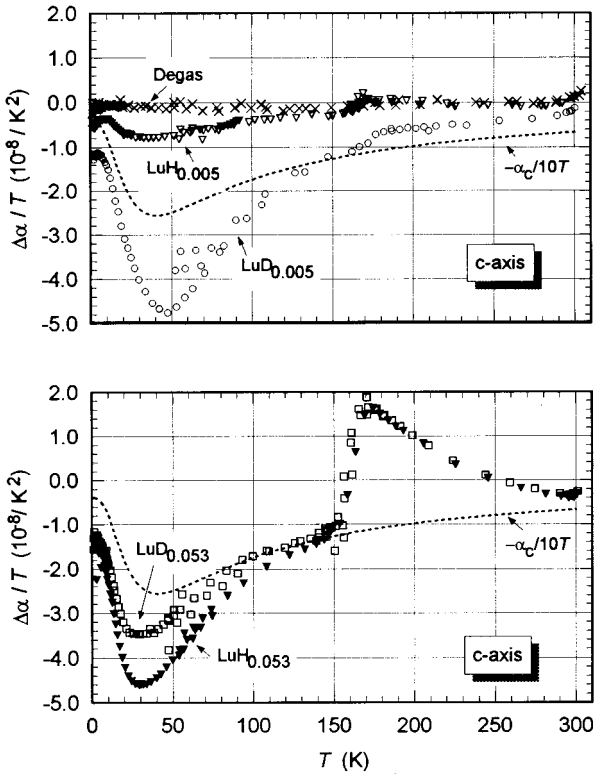

FIG. 8. $(\alpha-\alpha_{\text{pure}})/T=\Delta\alpha/T$ for the c-axis alloys in Fig. 6. A relative scale is given by the reduced smooth c-axis expansivity, $\alpha_c/10T$ (----).

parently are significant only for the a-axis crystals. A frequency- and temperature-dependent structure is found near these temperatures in internal friction studies.[42]

Relatively large systematic differences on warming and cooling (and hysteresis) were described above for the a-axis crystals above T_{tr}. The c-axis $LuD_{0.005}$ data in Figs. 7 and 8 show similar sample-related effects between 50 and 80 K, where data taken on cooling to 45 K lie significantly (2%) higher than those taken subsequently on warming from 45 K, although they coincide above 80 K. The sample then was cooled to 1 K, with the 50 K data taken on warming 4% smaller than the previous warming data from 45 K. Drifts in sample length which were observed on occasion at 25(5) K usually did not reappear after cooling to 1 K. The most consistent drifts in sample length occurred between 130 and 200 K for most of the alloys ($LuD_{0.005}$ was an exception). These generally were small (on the order of 1 Å/min) and had no significant effect on data taken over a period of 1 h or so. On cooling, the sample length would decrease rapidly due to the positive α, then would continue to shorten slowly after T became constant (after 1 h). The opposite effects were observed on warming. These effects varied in detail from sample to sample, and generalizations are difficult. Measured time constants were as short as a few hours or as long as 100 h. For the longest time constants, the projected changes in sample length were estimated to be -20 ppm for the c-axis and $+7$ ppm for the a-axis sample. These time constants introduce an ambiguity in the analysis of the data, since it is not clear whether α should be determined by the sample length change corrected back to the time when dilatometer equilibrium was reached, or to the projected long-time sample length. When small ΔT's were used in the transition region, this could result in α's which differed by as much as 10%. Possibly related effects were noted in neutron scattering experiments by Blaschko *et al.*[43] who reported that the intensity of a neutron diffuse scattering pattern for $LuD_{0.04}$ at 150 K increased by a factor of 2 in 24 h.

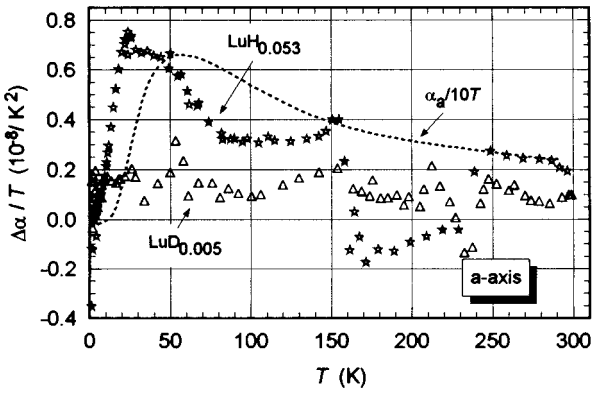

FIG. 9. $(\alpha-\alpha_{\text{pure}})/T=\Delta\alpha/T$ for the a-axis alloys in Fig. 6. A relative scale is given by the reduced smooth a-axis expansivity, $\alpha_a/10T$ (----).

IV. DISCUSSION

The present C_p data support the original conclusion[2,3,7] that the C_p's of α-phase Lu-hydrogen alloys (LuH_x) behave quite differently below 3 K for $x\leqslant 0.015$ and for $x\geqslant 0.032$ (Fig. 3). In addition, the present data show that any model which describes these C_p results must not depend significantly on the mass of the hydrogen isotope; this apparently eliminates models which involve motion of the hydrogen (such as tunneling). The H (D) which are paired along the c axis on either side of a Lu ion apparently are bound to the ion sufficiently well that lattice heat capacities, and the Debye temperature Θ_0, are related to the molecular weight, not the atomic weight, of the sample. The agreement between our $x=0.005$ alloy C_p data and those for the pure metal for $T>10$ K (Figs. 1 and 2) suggests a common Θ_0; Thome's LuH_x data for $x\leqslant 0.015$ (not shown) also are consistent with this postulate. For larger x, the small decreases in C_p with x in Figs. 1 and 2 (Table I) can be understood in terms of small increases in Θ_0 (Table I) which are consistent with those found in ultrasonic[18] and energy-dispersive x-ray[19] experiments on these alloys; the reduced representations in Fig. 4 suggest that the shape of the lattice relation is unchanged by alloying. Although the data for $x\geqslant 0.032$ (Fig. 3 and Table I) are consistent with an x dependence for the electronic C_p coefficient γ (which approaches the pure value for $x=0.183$), no evidence exists for similar effects for $x\leqslant 0.015$, where the low-temperature anomaly obscures this contribution.

The low-temperature linear expansivity data in Fig. 6 have strong isotope and x dependences, but for $x=0.005$ do not exhibit the same type of anomaly below 3 K as the C_p data (Fig. 3). The dilatometer may not be sufficiently sensitive to resolve these effects if, as the preceding paragraph suggests, tunneling does not occur.

While the "high-T" C_p data are relatively uninteresting, the same is not true for the corresponding α's. The rather broad "pairing transition" at T_{tr}, the magnitude of which appears to scale with x (Table II), clearly is evident in Figs. 5 and 7–9, as are pretransition effects. The T_{tr} are consistent with those from resistivity measurements, although conditions in the two experiments are quite different; the resistivity data are taken with a carefully chosen continuous warming or cooling rate of 0.5 K/min,[22] while our samples, due to the mass of the dilatometer, can only be warmed (or cooled) much more slowly, with an hour or so required for equilibrium near the transition. The nonequilibrium effects (isothermal drifts in sample length) which we observe do not appear to be important for the resistivity studies. The C_p data of Vajda *et al.*[24] for a $LuD_{0.183}$ crystal show broad feature in C_p at 203 K; resistance measurements on a similar sample showed a transition at 174 K (Table II).

Nuclear magnetic resonance studies have shown that the pairing transition is accompanied by a change in electronic structure.[23] Since electronic contributions to thermodynamic properties are proportional to T [the lead terms in Eqs. (1)], the plots of $\Delta\alpha/T$ in Figs. 8 and 9 are intended to emphasize differences between the electronic properties of the alloys and the pure metal. The two common features for the $x=0.005$ and 0.053 alloys are, first, that each shows a transition, the magnitude of which scales approximately with x (Table II), and second, that $\Delta\alpha/T$ in each case has similar structure below the transition (with different signs for the a-axis and c-axis alloys). These similarities are in contrast with the very different isotope dependences for the $x=0.005$ and 0.053 c-axis α's in Fig. 8, and with their very different pretransition temperature dependences. An intriguing feature in Fig. 8 for all four c-axis alloys is the correspondence between $\Delta\alpha/T$ at $T=0$ and at the low-temperature end of the transition; this, presumably, corresponds to the electronic structure change which is observed in the nuclear resonance data. The intermediate structure is large, and puzzling, since no resolvable isotope-dependent effects are observed in the C_p data for these temperatures (50 ± 25 K).

Our analyses of the C_p's and the α's for pure lutetium (and scandium) crystals[11] demonstrate that electronic effects are relatively much more important for the α's than for the C_p's. The "high-T" lattice properties of these crystals can be made consistent with lattice dynamical predictions only if the assumption is made that the very significant spin-fluctuation and electron-phonon enhancements to the electronic contributions for both C_p and α are quenched with increasing temperature. This is consistent with the suggestion by Grimvall[44] that spin-fluctuation (and electron-phonon) contributions should begin to disappear for $T>\Theta/10$. The electronic contributions each are proportional to T, with a different proportionality parameter [C_0 in Eq. (1a) for C_p, A_0 in Eq. (1b) for α] for low and high T and a complex intermediate behavior; the quenching of the enhancements has a relatively much smaller effect on C_p than on α.[11] Table III contains on the first line the low-temperature values of A_0 for pure Lu and the alloys, and on the second line the "high-T" value, A_{0b}, for the pure metal. Unfortunately, the consistency analysis does not give direct information as to the temperatures at which the quenching of the enhancements occurs.

In Figs. 8 and 9, the magnitude of the structure in $\Delta\alpha/T$ near 40 K is similar to that which is associated with the quenching of the enhancements for the pure metal (A_0-A_{0b}, Table III). This suggests that this structure in $\Delta\alpha/T$ vs T is associated with a more rapid quenching of the enhancements with increasing T for the alloys than for the pure material, as was suggested by Stierman and Gschneidner.[8] The almost identical values of $\Delta\alpha/T$ at $T=0$ and at the low-temperature end of the transition for each of the alloys then reflects the effect of the ordering on the bare density of states contribution to α, with the dominant enhancement contributions no longer present above 150 K. Similar effects which should occur for C_p would be relatively much smaller, and possibly would be indistinguishable from those in Figs. 1 and 2 which we have attributed to the x dependence of Θ_0.

With this postulate, the quenching of the enhancements for the c-axis alloys (when compared with the pure metal) is least effective for the $LuH_{0.005}$ alloy, appreciably more so for $LuD_{0.053}$, and most effective for $LuD_{0.005}$ and $LuH_{0.053}$; the isotope effect is reversed for $x=0.005$ and 0.053. If the quenching were complete for a c-axis alloy (but not initiated for the pure metal) near, for example, 10 K, the shape of the $\Delta\alpha/T$ vs T curve would reflect the temperature dependence of the quenching in the pure metal; $\Delta\alpha/T$ initially would decrease rapidly by 4.1×10^{-8} near 10 K (solely an alloy effect) and then would rise slowly to its $T=0$ value as the metal enhancements disappeared with increasing T. Figure 8 suggests that for the pure metal the major enhancement quenching occurs between 30 and 125 K (it does not scale with Θ when compared with scandium), and probably occurs between 10 and 50 K for the alloys, since the largest magnitudes for the change in $\Delta\alpha/T$ are $3.3(2)\times10^{-8}$. In Fig. 6, the gradual decrease in the average slopes of the smooth relations between 0 and 12.6 K could be related to the onset of enhancement quenching in the alloys.

The situation is less clear for the a-axis α's in Fig. 9, where no structure comparable with that for the corresponding c-axis crystal is observed for a-axis $LuD_{0.005}$ (where quenching is not enhanced?), and $\Delta\alpha/T$ for $LuH_{0.053}$ at the beginning of the 160 K transition is the same as that at $T=0$. The intermediate shape mirrors that for the c-axis crystal and is consistent with enhanced quenching of the enhancements for this alloy. For this alloy, the structure above T_{tr} does not reflect the smooth relationship for the same c-axis alloy. If the c-axis expansivities are characteristic of the c-axis pairing transition in these alloys, the a-axis data show that subtle anisotropic corollary effects occur. Possibly this reflects the relatively greater softness of the pairing potential normal to rather than along the symmetry axis.[26]

V. SUMMARY

The present results, rather than clarifying, increase the complexity of the experimental picture for thee $LuH(D)_x$ alloys. The original low-temperature C_p data for polycrystalline LuH_x samples[1–3] were consistent with the existence of two different states for these alloys, with a transition occurring for $0.015\leqslant x\leqslant0.032$; the lower-$x$ state is characterized by a C_p anomaly, while the larger-x state has a "normal" T dependence (Figs. 1–3). The present C_p data show that the low-temperature, small-x anomaly is not isotope dependent,

and, hence, cannot be associated with hydrogen motion such as would occur in tunneling. A corresponding anomaly does not appear in the $x=0.005$ linear thermal expansivity data, possibly because of a lack of dilatometer sensitivity.

The higher-temperature single-crystal thermal expansivity data also are consistent with the existence of two quite different states for these alloys, since the temperature dependences and isotope effects for the *c*-axis α's are quite different for $x=0.005$ and 0.053. The pairing transition at T_{tr}, which is observed in electrical resistivity experiments[22] and as a change in electronic structure in NMR data,[23] appears as a well-defined discontinuity in α at approximately the same temperatures (Figs. 5 and 7–9 and Table II) which is proportional to *x*. For the *c*-axis crystals, the change in the electronic contribution to α upon alloying $[\Delta\alpha/T=(\alpha_{alloy}-\alpha_{pure})/T]$ is the same at $T=0$ and at T_{tr}, and is believed to be associated with the electronic structure change observed in the NMR data. The large temperature dependence of $\Delta\alpha/T$ above T_{tr} for the *c*-axis crystals (Fig. 8) reflects the ordering of the H (D), while the abrupt decrease in α at T_{tr} indicates the termination of this ordering. An important question is whether the ordering triggers the electronic structure change, or whether the electronic structure change terminates the ordering.[45] Since the $\Delta\alpha/T$ which is associated with this change is approximately the same magnitude for the $x=0.005$ and 0.053 *c*-axis alloys, the latter postulate probably is more likely to be correct. A large isotope- and *x*-dependent anomaly in α which appears between $T=0$ and T_{tr} can be attributed to a more effective *T*-dependent quenching of spin-fluctuation and electron-phonon enhancements for the alloys than for the pure metal.

While the emphasis in the above paragraph has been on the *c*-axis expansivities, the *a*-axis data also are interesting in that they, too, reflect the transition, but with different detailed behavior. The α's for both *a*-axis samples ($LuD_{0.005}$ and $LuH_{0.053}$) showed hysteresis and structure above T_{tr} which did not appear in the comparable *c*-axis data. Whether this reflects different physics, or the relative softness of the H (D) potential in the basal plane, is not clear.

Questions which future experiments might answer are as follows.

(1) Is the ''change in character'' of the low-temperature C_p (Figs. 2 and 3) gradual, or does it occur at a distinct value of *x*? This probably would involve 1–20 K C_p data for a range of *x*, from 0.01 to 0.03; α measurements on *c*-axis crystals also would be useful.

(2) The present measurements should be extended to higher *x* values (at least to $x=0.183$, 15 at. %) to determine the *x* dependence of the α's and possible saturation effects.

(3) Alloy C_p measurements should be extended to higher temperatures to investigate the C_p anomaly which corresponds to those for α at and above T_{tr} (Figs. 5 and 7–9). Only one determination of an alloy C_p at these temperatures has been reported (Table II).[24] This will be a difficult experiment, and perhaps can be done best in a differential calorimeter as a direct comparison with pure Lu.

ACKNOWLEDGMENTS

Kenneth N. Hagen carried out the C_p measurements for the large polycrystalline sample which were crucial for determining the initial difficulties in these experiments. K. A. Gschneidner, Jr. kindly provided a copy of the thesis of D. K. Thome,[1] which contains a tabulation of the data for the LuH_x C_p's. Extremely useful conversations with B. N. Harmon and R. G. Barnes are gratefully acknowledged; the neutron diffraction study of the $LuD_{0.005}$ crystal by J. L. Zaretsky and C. Stassis gave needed assurance of crystal quality. The alloy samples were prepared and characterized in the Materials Preparation Center of the Ames Laboratory. This work was performed at the Ames Laboratory, Iowa State University and was supported by the Director of Energy Research, Office of Basic Science, U.S. Department of Energy under Contract No. W-7405-ENG-82.

[1] David Keith Thome, M.S. thesis, Iowa State University, 1977.
[2] D. K. Thome, K. A. Gschneidner, Jr., G. S. Mowry, and J. F. Smith, Solid State Commun. **25**, 297 (1978).
[3] K. A. Gschneidner, Jr. and D. K. Thome, in *The Rare Earths in Modern Science and Technology*, edited by G. J. McCarthy and J. J. Rhyne (Plenum, New York, 1978), pp. 75–79.
[4] T.-W. E. Tsang, K. A. Gschneidner, Jr., F. A. Schmidt, and D. K. Thome, Phys. Rev. B **31**, 235 (1985); **31**, 6095(E) (1985) (corrects Sc Θ to 345.3 K).
[5] B. J. Beaudry and F. H. Spedding, Metall. Trans. B **6B**, 419 (1975).
[6] J. N. Daou and J. E. Bonnet, J. Phys. Chem. Solids **35**, 59 (1974).
[7] K. A. Gschneidner, Jr., in *Science and Technology of Rare Earth Materials*, edited by E. C. Subarao and E. C. Wallace (Academic, New York, 1980), p. 25.
[8] R. J. Stierman and K. A. Gschneidner, Jr., J. Magn. Magn. Mater. **42**, 309 (1984).
[9] K. A. Gschneidner, Jr., H. Gnugesser, and K. Neumaier, Physica B+C **108B**, 1007 (1981).
[10] W. A. Taylor, M. B. Levy, and F. H. Spedding, J. Phys. F. **8**, 2293 (1978).
[11] C. A. Swenson, preceding paper, Phys. Rev. B **53**, 3669 (1996).
[12] H. Wipf and K. Neumaier, Phys. Rev. Lett. **52**, 1308 (1984)
[13] Hermann Grabert and Helmut Wipf, Festkörperprobleme **30**, 1 (1990).
[14] J. N. Dobbs, A. C. Anderson, T. H. Metzger, and H. Wipf, Phys. Rev. **30**, 6168 (1984).
[15] J. G. Collins, S. J. Collocott, R. J. Tainsh, C. Andrikidis, and G. K. White, Aust. J. Phys. **40**, 65 (1987).
[16] J. N. Dobbs, M. C. Foote, and A. C. Anderson, Phys. Rev. B **33**, 4178 (1986).
[17] J. J. Tonnies, K. A. Gschneidner, Jr., and F. H. Spedding, J. Appl. Phys. **42**, 3275 (1971).
[18] J. D. Greiner, B. J. Beaudry, and J. F. Smith, J. Appl. Phys. **62**, 1220 (1987).
[19] T. H. Metzger, P. Vajda, and J. N. Daou, Z. Phys. Chem. (Neue Folge) **143**, 129 (1985).
[20] J. Pleschiutschnig, O. Blaschko, and W. Reichardt, Phys. Rev. B **41**, 975 (1990).
[21] O. Blaschko, G. Krexner, L. Pintschovius, P. Vajda, and J. N. Daou, Phys. Rev. B **38**, 9612 (1988).

[22] J. N. Daou, P. Vajda, A. Lucasson, P. Lucasson, and J. P. Burger, Philos. Mag. A **53**, 611 (1986).
[23] R. G. Barnes, J. Less-Common Met. **172-174**, 509 (1991).
[24] P. Vajda, J. N. Daou, J. P. Burger, K. Kai, K. A. Gschneidner, Jr., and B. J. Beaudry, Phys. Rev. B **34**, 5154 (1986).
[25] P. Vajda, J. N. Daou, P. Moser, and P. Remy, J. Less-Common Met. **172-174**, 522 (1991).
[26] O.Blachko, J. Less-Common Met. **172-174**, 237 (1991).
[27] N. F. Berk, J. J. Rush, T. J. Udovic, and I. S. Anderson, J. Less-Common Met. **172-174**, 496 (1991).
[28] M. W. McKergow, D. K. Ross, J. E. Bonnet, I. S. Anderson, and O. Schaerpf, J. Phys. C **20**, 1909 (1987).
[29] I. S. Anderson, J. J. Rush, T. Udovic, and J. M. Rowe, Phys. Rev. Lett. **57**, 2822 (1986).
[30] T. J. Udovic, J. J. Rush, I. S. Anderson, J. N. Daou, P. Vajda, and O. Blaschko, Phys. Rev. B **50**, 3696 (1994).
[31] Feng Liu, M. Challa, S. N. Khanna, and P. Jena, Phys. Rev. Lett. **63**, 1396 (1989).
[32] S. E. Weber, Feng Liu, S. N. Khanna, B. K. Rao, and P. Jena, J. Less-Common Met. **172-174**, 485 (1991).
[33] O. Blaschko, Phys. Rev. Lett. **65**, 1168 (1990).
[34] Yan Chang and M. Y. Chou, Phys. Rev. B **49**, 13 357 (1994).
[35] B. J. Min and K.-M. Ho, Phys. Rev. B **40**, 7532 (1989).
[36] B. J. Min and K.-M. Ho, Phys. Rev. B **45**, 12 806 (1992).
[37] J. L. Zaretsky and C. Stassis (private communication).
[38] M. S. Anderson and C. A. Swenson, Rev. Sci. Instrum. **49**, 1027 (1978).
[39] C. A. Swenson, in Thermal Expansion of Solids, edited by R. E. Taylor, CINDAS Data Series on Material Properties Vols. 1–4 (CINDAS/Purdue, West Lafayette, in press), Chap. 8.
[40] E. S. R. Gopal, *Specific Heats at Low Temperatures* (Plenum, New York, 1966).
[41] J. N. Daou, A. Lucasson, and P. Lucasson, Solid State Commun. **19**, 895 (1976).
[42] P. Vajda, J. N. Daou, and P. Moser, J. Phys. (Paris) **44**, 543 (1983).
[43] O. Blaschko, G. Krexner, J. Pleschiutschnig, G. Ernst, J. N. Daou, and P. Vajda, Phys. Rev. B **39**, 5605 (1989).
[44] G. Grimvall, *The Electron-Phonon Interaction in Metals*, edited by E. P. Wohlfarth, Selected Topics in Solid State Physics Vol. 6 (North-Holland, New York, 1981).
[45] R. G. Barnes (private communication).